Electrochemical and XAS analysis of the ruthenium-dioxide material, and its application for Dimensionally Stabilized Anodes

Sujit K Mondal[a‡], Badri Shyam[b], Andrea F Gulla[c] and Sanjeev Mukerjee[a*]

[a]*Department of Chemistry and Chemical Biology, Northeastern University, Boston, MA-02115, USA.*

[b]*Department of Chemistry,George Washington University, Washington, USA.*

[c]*DeNora Tech, Chardon, Ohio-44042, USA.*

‡*Present affiliation in School of Engineering and Applied Science, Harvard University, USA.*

Corresponding authors. Tel: +1617 495 4469

E-mail address: sujit@seas.harvard.edu (S. K. Mondal).

Abstract

This manuscript represents an investigation of structure, property and electrochemical activity for commercially available RuO_2 coated titanium electrode, known as DSA. The investigation mainly aimed at XAS studies to understand the hidden structural information for RuO_2. A thick (150 micron) and a very thin (6 micron) titanium metal coated with RuO_2 was exposed at ex-situ and in-situ XAS experiment to find out its electrocatalytic property and corrosion during chlorine generation reaction. A detailed survey of XANES and EXAFS showed that the stable RuO_2 formed a nano cluster during chlorine generation reaction and this clusters produced a distorted rutile structure for RuO_2 with an enhanced electrocatalytic activity.

Introduction

Four decades have elapsed since the instant when the first titanium anodes with a metal oxide active coating, known as dimensionally stable anodes (DSA), were created. Among these anodes, the electrodes with coatings based on mixed ruthenium and titanium oxides (ORTA) and the latter with additives of doping oxides of non-noble metals with partial or complete replacement of ruthenium oxides of other noble metals in their coatings enjoyed extensive practical application. By now these anodes practically and completely replaced the graphite anodes that had been used in the chlorine industry. This was due to the fact that they substantially exceed the latter by their catalytic activity, selectively, and corrosion resistance. The presence of such characteristics of anodes explained the tremendous interest that was exhibited in studying the corrosion and electrochemical behavior of anode of this type. As a result of performed investigations, kinetics was studied and the mechanism of the evolution of chlorine and oxygen was established.

From the literature survey we found that scientists have used RuO_2 rutile phase oxide material for both chlorine and oxygen generation reaction. Scientists have already tried other oxide material to replace the RuO_2 but they found that the activity (performance) was one the main issue related to the oxide material [1]. The different values of tafel slope was reported during chlorine generation reaction by varying the calcinations temperature and also by changing the concentration of chloride containing electrolyte [1,2]. RuO_2 become more interesting material as it shows some high electroctalaytic property and high stability during chlorine generation reaction. Scientists have also used mixed oxide [1] for DSA but the best results obtained for RuO_2 and that's the main reason scientists are interested to explore DSA by using the RuO_2 catalyst.

Moreover, it was also found that very few reports were available for electrochemical impedance spectroscopy, which was not directly related to catalyst (RuO_2) here in this manuscript a logical conclusion was derived from electrochemical impedance study of RuO_2 during chlorine oxidation reaction. The main active material for DSA was RuO_x (nominally RuO_2). It was routinely prepared by thermal decomposition of $RuCl_3$ nH_2O (with n= 2, 3) so that chlorine remained in the oxide

during the preparation route. The chlorine content decreases as the time of calcinations increases. Under practical conditions, its concentration may be an order of a few weight percent [2].

Reports about EIS technique for the RuO_2 material had been found on rotating ring disc electrode [3] and RuO_2 nanoneedles on glassy carbon electrode [4], but we used the direct catalyst material coated over titanium for studying chlorine oxidation reaction by electrochemical impedance spectroscopy to understand the double layer capacitance and charge transfer resistance, these parameters were obtained by fitting with the software available from Autolab Instrument. We were able to give new information about the oxide material, mainly for RuO_2 coated over 2 different thickness of titania. XAS experiment also showed some interesting phenomenon in the formation of RuO_2 nanoclusters of both dimers and trimers on the Ti surface during chlorine generation reaction, gave rise to the specific catalytic properties of RuO_2 sample. In this manuscript we are trying to co-relate the structure property relationship for RuO_2 during chlorine generation reaction and trying to answer the following questions, which are till not being answered properly to the best of author's knowledge.

1) Can it possible to coat RuO_2 over very thin titanium metal such as 6 micron and 30 micron to study in-situ XAS technique? Reported values of dimension for Ti available in between 100 to 200 micron.
2) Can it possible to resolve the tafel slope particularly for Chlorine generation reaction?
3) Can it possible to evaluate the diffusion coefficient of the electrolyte during potentiodynamic method?
4) Can it be possible to co-relate the structure property relationship from In-situ and Ex-situ XAS studies for RuO_2 during chlorine generation reaction?
5) Is it really the rutile phase of RuO_2 responsible for its higher electrochemical activity?

A detailed analysis and understanding of the above mentioned questioned has been explained in the following manuscript.

Experimental

Electrodes were prepared by thermal decomposition of solution containing ruthenium ion and spread over titanium and subsequently dried at 500 ^{0}C. The titanium substrate was cleaned with organic solvent and etched with dilute HCl before coating. Then catalyst coating was prepared by sequential addition of catalyst solution using paint brush over pretreated titanium substance. Several layers were coated over the titanium substance to have the desired catalyst loading, but every intermediate layer was fired at 500 ^{0}C for 10 minute before the next layer was formed by coating. The dimension of the titanium was fixed to (1.0 X 1.0) cm^2. To follow up chlorine oxidation reaction in sequence the experiments were carried out in two different titanium current collectors coated with RuO_2. The sample loading level for 150 micron was 15 mg cm^{-2} and 6 micron was 20 mg cm^{-2}.

All the electrodes were used for cyclic voltammetry experiments. A three electrode glass cell was assembled and used for cyclic voltammetry experiment. Argon gas was purged for 20 minute to the electrolyte solution to make it an oxygen free medium. Working potential window for ruthenium di-oxide was experimentally evaluated depending upon the hydrogen and oxygen generation reactions. The ruthenium di-oxide showed its characteristic voltammograms with a high double layer charging. The capacitance was calculated and plotted as a function of scan rate. From the modified Randles-Sevick plots the diffusion coefficient for chloride ion was calculated. The cyclic voltammetry experiments were performed for RuO_2 electrode in 0.5(M) Na_2SO_4 and 0.07(M) NaCl solution with Ag/AgCl as the reference electrode. The two different sample specimens for RuO_2 (over 150 micron and 6 micron titanium) were prepared for SEM experiment. Due to the morphological features, the RuO_2 electrode was referred as 'mud cracked morphology'.

Chlorine evolution was chosen as the reaction to evaluate the electrocatalytic property because of its high sensitivity to surface modifications of titanium by RuO_2. Quasi-steady state kinetics measurement was carried out by conditioning the RuO_2 electrode at 1.15 V for 5 minutes then by incrementing the potential anodically in 50 mV steps and reading the current after 5 minutes of polarization up to a potential of 1.6 V

(Chlorine evolution potential) with respect to Ag/AgCl electrode, no hysteresis was observed. Two different electrodes coated with RuO_2 were subjected to perform the steady state experiment to follow up the tafel slope for chlorine evolution reactions.

These electrodes were also used to perform electrochemical impedance spectroscopy experiment. The three electrode configuration cell was set up for EIS experiments. The AC impedance experiment was carried out with a wide frequency range starting from 100 kHz to 10 mHz range. The EIS experiments for RuO_2 electrode were performed by conditioning the electrode at 0.8 V (before chlorine generation potential) to a high potential of 1.4 V (beyond chlorine generation potential) with respect to Ag/AgCl electrode. The highly scattered data were obtained at a lower frequency region for RuO_2 electrode for the EIS (Nyquist diagram) when the measurement was carried out 1.4 V due to chlorine generation reaction. The Nyquist diagram was obtained for these electrodes with a wide frequency range starting from 100 kHz to 10 mHz. Due to vigorous chlorine evolution at 1.4 V the spectrum was having scattered region. All the EIS spectra were fitted with the Autolab software.The electrode potential was read against Ag/AgCl as reference electrode for Na_2SO_4 + NaCl mixed solution for RuO_2 electrode.

The XAS ex-situ experiments were performed for the RuO_2 sample coated over 150 micron titanium. X-ray absorption spectroscopy data on the samples were collected at the National Synchrotron Light Source, Brookhaven National Lab, Upton NY at beamline X-11A. All data were collected at the Ru K-edge in transmission mode. The data consisted of spectra for two samples, one cycled to a potential *below* that at which no chlorine evolution, (sample II) and the other, to a potential *above* the chlorine evolution potential (sample I). Both spectra were collected *ex-situ* in air, at room temperature (22 ºC). The In-situ experiments were performed over 6 micron titanium substrate coated with RuO_2 at various potential ranges starting with 0.65V, below the chlorine evolution and above the chlorine generation potential eg. 1.5V, all the potential values were measured with respect to Ag/AgCl.

Results and Discussion

1) Dynamic method

a) Cyclic Voltammograms for RuO_2 electrode: Cyclic voltammograms for RuO_2 were also very interesting, at first we observed oxygen generation (1.1 V) followed by chlorine evolution potential at 1.2V and also hydrogen evolution at almost 0.0 V versus Ag/AgCl electrode, it was shown in Fig.1. Depending upon these the working potential window for RuO_2 is 0.0 V to 1.0 V with respect to Ag/AgCl electrode was evaluated for non faradaic reaction and beyond 1.0 V for faradaic reaction. The cyclic voltammetry experiments were performed with various scan rates in non faradaic reaction zone, as shown in Fig.2, a typical capacitor type voltammogram which closely resembles RuO_2 with mud-cracked morphology. The voltammograms were almost symmetrical in nature and this was specifically due to redox related charging and sodium ion diffusion into cracked sites and interstitial sites of RuO_2. This phenomenon was observed for all the 2 substrates of titanium coated with RuO_2 irrespective of the thickness. The maximum anodic current value 0.5 mA per cm^2 (geometric area) was obtained for 10 mVs^{-1} scan rate for RuO_2 in coated over 150 micron titanium sheet. From Fig.3 the plot of anodic charge versus scan rate showed a almost linear behavior for both the two titanium metal coated with RuO_2. Linear relationship between anodic charge and scan rate, due to diffusion controlled reaction for oxide catalyst and also diffusion of sodium ion (as sodium ion present in the electrolyte) was probable case inside the oxy-hydroxy layer as a function of potential [5]. The number of electrons was determined to be 2 for this anodic reaction. So the probable oxidation state of Ru is (+ 4) in RuO_2, using Randles-Sevick equation and diffusion coefficient of Sodium ion in aqueous medium was evaluated and $D = 2.032 \times 10^{-5}$ cm^2 s^{-1} [7] matched with reported literature value.

$$I_p = (2.69\times 10^5)\, n^{3/2}\, C_0^{\infty}\, D^{1/2}\, \gamma^{1/2} \qquad (1)$$

The higher values for the charge and capacitance were observed for the 6 micron titanium substrate coated with RuO_2 was only because of the 6 micron titanium having smaller particle size of RuO_2 and higher electrochemical active sites for chloride ion adsorption over catalyst. From the SEM mud-cracked morphology was found for RuO_2 and showed in Fig.5. The cracks were manifestation of macro roughness, while pores constituted micro roughness. This type of morphology supported the diffusion process for sodium ion and hence the behavior of high capacitance values was obtained. In case of RuO_2 very high capacitance was obtained (calculated from voltammetric measurements), almost

48mF cm^{-2} (per geometric area) for 6 micron titanium coated with RuO_2. The high value of capacitance was due to the redox charging and easier cation diffusion into defect sites and interstitial sites (mainly macro roughness and micro roughness) [3].

2) Steady State Phenomenon:

Steady state phenomenon named as chrono technique, this technique was employed to study the kinetics related to oxygen and chlorine evolution reaction across a particular potential range. The chronoamperometry experiment was performed for RuO_2 electrode to find out tafel slope for chlorine evolution reactions. For chlorine evolution reaction the chronoamperometry experiments was performed for two different thickness of titanium current collector coated with RuO_2 such as 150 micron and 6 micron and the chorno results for 150 micron and 6 micron titanium were shown in Fig.4, the starting point of the reaction was from 1.15 V up to 1.6 V, at which the vigorous chlorine evolution was observed. The following current values was transformed to a logarithmic scale to plot the Tafel equation (2) and a Tafel slope of 42 mV was calculated for chlorine generation reaction for 150 micron and 6 micron titanium. The close values of tafel slope for 2 different current collector showed that the mechanism for chlorine generation reaction was independent on thickness of titanium. This value was in agreement with the literature value [1].

$$\text{Log } I = \text{Log } I_0 + \alpha_A nF\eta/2.3RT \qquad (2)$$

4) AC Technique

Electrochemical Impedance Spectroscopy: The AC technique, electrochemical impedance spectroscopy, is a useful tool to investigate the charge transfer process (faradic reaction) at electrode-electrolyte interface, double layer capacitance, diffusion controlled electrode kinetics and non-faradic reaction related to psedocapacitive property. Nyquist plot explaining all these processes properly with respect to frequency range was shown in Fig.6 as model diagram. The f_{max} was the maximum frequency essential to calculate the double layer capacitance. In Nyquist spectrum double layer capacitance, faradaic process and Warbug component were the most important features. A non-faradaic process involves the accumulation of charges at the metal/solution interface then followed by charge transfer process (faradaic reaction). The plot of double layer

capacitance and charge transfer resistance with different potential showed a decrease in trend for RuO_2 catalyst, were shown in Fig.8. The double layer capacitance and charge transfer resistance and capacitance due to diffusion process were calculated by fitting the Nyquist spectra in AUTO lab software.

The impedance spectra for RuO_2 material at potential 0.8 V with respect to Ag/ AgCl electrode was obtained and plotted in Fig.7 for 150 micron titanium current collector. The charge transfer process for electrode-electrolyte surface was represented by a semicircle at higher frequency region. A straight line at lower frequency region with an angle around 45^0 to the real axis represented diffusion controlled kinetics, known as the Warburg component, and the sharp increase of the spectrum after the Warburg component was representative of the pseudocapacitive behavior of the material, mainly due to diffusion of ions. Impedance measurement was performed with wide range of frequency starting from 100 KHz to 10 mHz with various potential values for the RuO_2. A detailed circuit analysis was carried out with appropriate fitting with respect to EIS measurements. All the spectrum were fitted with the non linear least square fit available in AUTOLAB software in order to determine the C_{dl}, R_{ct}, and constant phase element.

$C_{dl} = (1/2\pi f*R_P)$ (3)

Double layer capacitance was calculated for RuO_2 material via fitting with non linear least square program available in the AUTO lab software. The high double layer capacitance was obtained from impedance spectrum due to double layer charging, and diffusion of the ions into defect sites and interstitial sites. The EIS (Nyquist) measurements were carried out at various potential values starting at 0.8 V to 1.4 V with respect to Ag/AgCl electrode. The typical Nyquist plot for RuO_2 material at potential 0.8 V and potential 1.4 V, was shown as in Fig.7. From the analysis of the impedance studies it was observed a steady decrease of charge transfer resistance (R_{ct}) for RuO_2 with an increase in potential values starting from 0.8 V to 1.4 V as shown in Fig.8. This is due to chloride discharge and simultaneous chlorine adsorption coupled to the double layer capacitance of RuO_2 [2]. The charge transfer resistance for 6 micron titanium is small compare to 150 micron titanium current collector. The probable reason was 6 micron titanium had more roughness factor than 150 micron titanium RuO_2, which lead to a more facile chloride ion adsorption over oxide surface and produced higher catalytic activity

($2Cl^- \rightarrow Cl_2 + 2e$). The spectra contain a semi circle (R_{ct}) at the higher frequency region followed by a spike at 45^0 angle with the real axis of Z at lower frequency, known as the Warburg component. A sharp increase with linear spike at lower frequency region after the Warburg component resembles the pseudo-capacitance for faradaic reactions. A decreasing trend in double layer capacitance was shown in shown in Fig.8 reason behind it was due to the adsorbed chloride ions were evolved as chlorine gas at the interface therefore effective electrochemical surface area of the catalyst was opened with less number of absorbed chloride ions, once the chloride oxidation took place ion association at the double layer would fall down. [2]. The whole reactions was carried out in 0.07 (M) NaCl + 0.5(M) Na_2SO_4 solution with a titanium as counter electrode with respect to Ag/AgCl as reference electrode. The maximum potential value used for the impedance studies for RuO_2 material is 1.4 V, this means almost 1.6 V normalized with respect to normal hydrogen electrode as the reference. The reason for not using much higher potential beyond 1.4 V was due to scattered data points for vigorous evolution of chlorine gas. The maximum value for double layer capacitance was obtained, 360μF at 0.8 V for 150 micron and 300μF for 6 micron titanium coated RuO_2. The value reached a minimum of 75 μF at 1.4 V potential with respect to Ag/AgCl electrode. For the both the material the solution resistance obtained was in good agreement. The little deviation of the solution resistance could be the change in position of reference electrode with respect to working electrode.

4) XAS Technique

The XANES region: All data were processed using the IFEFFIT suite [8-10] (v.1.2.9). The scans were first normalized between 0 and 1 for XANES analysis and the reference scans of the samples were calibrated and aligned to the standard Ruthenium K-edge (22117 eV)[11]. The shifts thus observed represent the actual shift in the edge energy due to the oxidation state of Ruthenium in the samples. Fig.9 showed the XANES region for the two samples and a standard Ruthenium foil, which was expected to be in its elemental state, viz. Ru(0). The edge energy for samples I and II were located at 22123.72 eV and 22125.87 eV. The most apparent difference between the two samples is the difference in the white-line intensity of the main peak centered around 22140 eV. The higher intensity in the case of sample I indicates that this sample is oxidized to a larger extent than sample

II. It correlated well with the fact that sample I was cycled to a higher potential than sample II and thus suggests a clear, local morphology change between the two samples. These changes are discussed in greater detail in the section that follows.

Sample 1	Ru-O	Ru-Ru (1st Shell)	Ru-Ru (2nd Shell)
Amp	7.08 (0.6)	0.87 (0.24)	3.19 (0.56)
ΔE (eV)	-32.12 (4.4)	25.76 (5.85)	16.00 (0.100)
r (Å)	1.955 (0.016)	2.564 (0.029)	3.398 (0.009)
σ^2 (Å ^{2})	0.0041 (0.004)	0.0043 (0.012)	0.004

Sample 2	Ru-O	Ru-Ru (1st Shell)	Ru-Ru (2nd Shell)
Amp	5.21(0.42)	0.57 (0.19)	2.22 (0.37)
ΔE (eV)	-28.97 (4.42)	31.31(6.648)	17.61 (0.101)
r (Å)	1.961 (0.016)	2.596 (0.034)	3.399 (0.009)
σ^2 (Å^2)	0.0041 (0.004)	0.0043 (0.012)	0.004

Table 1. Ru EXAFS First and second shell fits on both samples I and II using Ru-O and Ru-Ru paths

EXAFS Analysis: The data were processed to obtain the oscillatory chi(k) function by removing the background above the edge and was fit using the standard procedure used in EXAFS analysis. Briefly, the energy in electron volts (eV) was converted to k-space over the region from 2 to13.25 Å^{-1}. The data were then k^2-weighted and Fourier-transformed to produce a partial radial distribution (RDF) function around Ruthenium. The fits were carried out in the region 1.193 Å < r < 3.633 Å using a Kaiser-Bessel window spanning this data range in r-space. The partial radial RDFs of the samples were analyzed using the FEFF code (v. 6.0) incorporated in the program ARTEMIS [12] to obtain average bond distance (r), coordination number (n) and the Debye-Waller factor (σ^2) for the nearest Ru-O and Ru-Ru neighbors. In all, three paths (1 Ru-O and 2 Ru-Ru) were fit to the samples using the four standard parameters for each path viz., the amplitude (S_0^2), energy (ΔE), radius of path (Δr) and the Debye-Waller factor (σ^2), which was a measure of thermal disorder in the samples. All fits were carried out in r-space and

the fits for samples I and II were shown in fig. 12 and 13 respectively. The comparison of pseudo radial distribution function and oscillatory chi(k) function for both samples with Ru foil were described in Fig. 10 and Fig. 11. The results of the fits were shown in Table 1.

Discussion of results: From the XANES region (Fig.9), it is seen that the Ruthenium in sample I is oxidized to a larger extent than that in sample II. This is seen in both, the edge energy shift ($\Delta E \sim 2$ eV) between the two samples and in the white line intensity. Although the overall shift in energy from that of Ru^0 is close to that found for Ru^{4+} (22.126 keV), McKeown et.al.[14] show that it is difficult to distinguish between Ru^{3+} and Ru^{4+} in ruthenium oxides from just the XANES region. It is thus possible that there is a certain fraction of both oxidation states in the samples.

The data was initially fit using an anhydrous, crystalline RuO_2 (Ru^{4+}) cluster wherein each Ru^{4+} ion in the RuO_6 octahedral was bonded to four oxygen ions at a distance of 1.984 Å and two axial oxygen ions at a distance of 1.942 Å. However, the fits were of poor quality. This could be due to one of the following reasons –

i. The samples I and II do not possess a perfectly rutile-like RuO_2 environment.

ii. The data quality and range over which the analysis was carried out limits the bond distance resolution to ca. 0.2 Å and thus, the fits with the two oxygen distances separated by under 0.05 Å does not yield good fits with acceptable parameters.

From observing the XANES region of the spectra and comparing it with those available in the literature [13-18], it is more likely that the samples are unlike standard RuO_2. The results from the fits indicate that the Ru (n^+) ions are present in an octahedral environment and surrounded by around 6 oxygen ions at a distance of ca. 1.95-1.96 Å. The bond distance obtained is intermediate to the Ru-O distances in RuO_2. The Ru-O coordination increases for the more highly oxidized sample I and is consistent with XANES results. The nearest significant Ru-Ru coordination seems to be at ca. 3.4 Å, which is considerably larger than the closest Ru-Ru distance in RuO_2 at 3.107 Å. This peak representing Ru-Ru scattering is quite broad and suggests a distribution of Ru-Ru nearest neighbor distances.

The fit between 2-3 Å is not very good and could be due to the interaction of Ru with the Ti substrate. As a first attempt in understanding this catalyst structure, including too many paths was avoided to minimize complexity in the analysis and interpretation of fit results. Attempts to reveal the exact local structure were in progress and involve comparisons with other known standards of ruthenium compounds in various oxidation states and environments.

In-situ XAS Analysis: The in situ data discussed in this section were collected at the Ru K-edge in fluorescence mode using a standard PIPS detector and sample used was RuO_2 coated over 6 micron titanium foil.

XANES analysis –

Fig.14 XANES region of spectra collected at various potentials including on set before and after chronoamperometric (CA) studies (data at 1.2V). The in-situ data collected in the XANES region was interesting in that there was virtually no change in the spectra across the various potentials. The data indicates that the material is in the same oxidation state, i.e. highly oxidized state at all potentials was investigated. This was not surprising given that the material being investigated was primarily RuO_2 and was thus expected to be fully coordinated to oxygens and likely independent of the applied potential. An edge shift of ca. 8.6 eV from that of the foil (Ru^0) is observed. On comparing the XANES region with spectra of standards in the literature (ref.) an overall oxidation state between 3 and 4 seems very likely as the shape of the white-line seems to be in between that of $Ru(Ac)_3$ and RuO_2.

EXAFS analysis –

Fig.15 and Fig. 16

The raw data in k-space are shown in Fig. 16. The data were analyzed between $2 < k < 13.95$ Å^{-1} and $1 < r < 3.579$ Å. A k-weight of 2 was used for all the fits. The pseudo-radial distribution function showing the data transformed into r-space are shown in Fig.15. The large peak centered on 1.6 Å was due to backscattering from the oxygen atoms present in the first shell of the RuO_2 catalyst particles. There seems to be little or no change in the Ru-O coordination with increase in potential between 0.65V and 1.2V. Further, the coordination didn't seem to change noticeably even after chronoamperometric studies at 1.2 V for 15min, suggesting that the material is quite

stable to electrochemical corrosion at high potentials. This peak however did increase in intensity slightly for the data at 1.5V due to increased oxidation of the material.

As seen previously in the ex-situ data, the region between 2-3 Å is somewhat complicated and therefore, unclear. The peak at 2.2 Å is most probably due to a longer Ru-OH bond distance (ref.) while the peak between 2.6-2.8 Å appears to be due to first shell Ru-Ru backscattering as it decreased slightly with potential, possibly due to increased Ru-O coordination (or Ru-Cl). A very interesting feature of the spectra at 1.2 V (after CA study) and 1.5V when compared with the other spectra at lower potentials is the appearance of a small peak at ca. 2.0 Å. This peak is suspected to be due to Ru-Cl scattering and is therefore only expected at higher potentials and after significant evolution of chlorine gas from chloride ions, whereby Cl^- species participated in diffusion through the material causing some Ru-Cl scattering. In the data at 1.5V, it was only a small shoulder whereas at 1.2V after the CA study, it was a small, though distinct peak because at 1.2 V continuous chlorine generations reaction was happened for 15 minutes.

The peak around 3.1 Å is most definitely due to Ru-Ru scattering at a distance of 3.58 Å as seen in anhydrous $Ru(OH)_2$. There is no change with potential indicating that any changes with potential are chiefly occurring within the first shell (below 3 Å) of the catalyst material. The spectrum at 0.65 V. and 1.5 V has been fitted with the Artemis software and results were tabulated in the following table. Fitted spectrum obtained from 0.65 V was described in Fig.17. It was clear from the table that there was a considerable amount of increase in co-ordination number from 0.65 V to 1.5 V which reflected the formation of $(Ru\text{-}O)_n$ nano cluster and thus enhancement of the catalytic activity for RuO_2 catalyst coated over titanium metal.

Sample 0.65V	**Ru-O**	**Ru-Ru (1st Shell)**	**Ru-Ru (2nd Shell)**
Amp	**1.64 (2Theoretical)**	**0.68 (2Theoretical)**	**0.6 (8 Theoretical)**
ΔE (eV)	**10.37**	**-10.35**	**10.2**
r (Å)	**1.91 (1.913Theoretical)**	**3.11 (3.11Theoritical)**	**3.54 (3.55 Theoretical)**
σ2 (Å2)	**0.008**	**0.0085**	**0.004**

Sample 1.5V	Ru-O	Ru-Ru (1st Shell)	Ru-Ru (2nd Shell)
Amp	7.72(2Theoretical)	1.335(2Theoretical)	1.2(8 Theoretical)
ΔE (eV)	10.3	-16.47	-10.2
r (Å)	1.8 (1.911Theoretical)	3.019 (3.11 Theoretical)	3.53 (3.55Theoretical)
σ2 (Å 2)	0.006	0.0069	0.002

Conclusions:-

1) The results reported in this manuscript clearly suggested that the electrochemical activity of RuO_2 originated from its specific crystalline nature and defect in the structure. The cyclic voltammograms showed a high capacitance, this was due to the sodium ion diffusion into the cracks and also possibly for redox charging ($RuO_2 + 2H+ +2e \leftrightarrow Ru_2O_3 + H_2O$).
2) The steady state polarization measurements for chlorine evolution reactions were carried over for RuO2 coated over 150 micron and 6 micron titanium. Tafel slope of 56mV was obtained for RuO_2 material. Values of the tafel slopes were almost comparable for both the 2 different thickness of titanium coated with RuO_2 material. We believe the tafel slope was influenced by oxygen generation reaction and from the tafel plot we were able to distinguish the slope between primary oxidative current and saturation limited current due to long range mass transport phenomenon. We were not able to separate out particularly the slope for chorine generation reaction as the electrochemical reaction was influenced by long range mass transfer process and also probably by oxygen generation reaction at the starting point.
3) Impedance spectra showed a high double layer capacitance for RuO_2 materials. In case of RuO_2 the high capacitance was due to the sodium ion diffusion cracks and also through the pores generated by mud crack morphology for RuO_2 material,

this morphology was confirmed by the SEM experiment. The particle size was small for 6 micron titanium compare to 150 micron titanium which reflects low charge transfer resistance. The surface roughness factor was higher in case of 150 micron titanium current collector and this reflected a very high double layer capacitance (ion- association at the electrode-electrolyte interface was higher due to facile adsorption) compare to the 6 micron titanium current collector coated with RuO_2 catalyst. Moreover, both the substances showed a comparable solution resistance value in EI spectrum.

4) From ex-situ XAS study we found that the primary difference between the two samples I and II, sample I was oxidized to a larger extent than sample II. This information was clearly visible from both, the XANES region and the EXAFS analysis and was consistent with the experimental treatment of the samples too. In the RDF of the samples, there were no multiple scattering peaks beyond ca. 6 Å which was characteristic of nanoparticle clusters of atoms. For both the samples, the RDF showed a high overall coordination number and it was 7-8 as obtained from the EXAFS analysis, the clusters were expected to be no larger than 5-6 nm. It is interesting to note that in the case of sample I, *both* the Ru-O and Ru-Ru coordination increase, suggesting that the particles have increased in size due to aggregation. It is thus possible that the RuO_n nanoclusters may be in the form of dimers or trimers on the Ti surface, giving rise to the specific catalytic properties of these samples.

5) In-situ XAS results also showed a direct co-relation with the ex-situ results, we found from the fitting parameters that significant increase in the co-ordination number for the sample which was oxidized at very high potential during in-situ chlorine generation reaction compare to the sample at lower potential where there was no evolution, this in fact certainly confirmed once again the formation of Ru-O_n nanocluster which was responsible for the higher catalytic activity for RuO_2. From the EXAFS a distinct peak was observed at 2.0 Å, which we believed that the formation of $[Ru(OH)Cl]^{-2}$ complex at the high potential of chlorine generation.

Acknowledgement:- Author SKM acknowledges DeNora Tech for funding and Nagappan Ramaswamy and T Arruda for their support during data collection in Brookhaven National Lab. Special thanks to Brookhaven National Lab for NSLS facility to carry out ex-situ and in-situ XAS study. Lastly author's greatest gratitude to Prof Sanjeev Mukherjee for his help and guidance.

References :-

1) S. Trassati et al Electrochim Acta 1984 29 (11) 1503-1512.
2) S. Trassati et al J. Electrochem. Soc **1989** 136 (5) 1545-1549.
3) Feng-Bin Li et al. Electrochimica Acta **1992** 37 (15) 2715 – 2723.
4) Mahima Subhramannia et al. J. *Phys. Chem. C* **2007**, 111, 16593-16600.
5) J. Mol. Phys **1989** 68 (4) 803-22.
6) A. J. Bard; L. Faulkner, *Electrochemical methods: Fundamentals and Applications;* Wiley: New York, **2001**.
7) Q. Huang; X. Wang; Li, J. Electrochim. Acta **2006**, 52 1758.
8) Hand Book of Chemistry and Physics. 77th ed. **1996-1997** CRC press.
9) M. Newville J., *Synchrotron Rad.,* **2001**, 8, 22.
10) Rehr et.al., *J. Am. Chem. Soc.,* **1991**, 113, 5135.
11) de Leon et.al., *Phys. Rev. B,* **1991**, 44, 4146.
12) Fuggle and Martensson, *J. Elect. Spect.*, **1980**, 21, 275.
13) Ravel, B. and Newville, M., *J. Synchrotron Rad.,* **2005**, 12:4, 537.
14) McKeown et.al., *J. Phys. Chem. B*, **1999**, 103, 4825.
15) Mo et.al., *J. Phys. Chem. B,* **2000**, 104, 9777.
16) Zhan et.al., *J. Am. Chem. Soc.,* **2003**, 125.
17) Ketchie et.al., *Chem. Mater.,* **2007**, 19, 3406.
18) Altwasser et.al., *Microporous and Mesoporous materials*, **2006**, 89, 109.
19) Caravati et.al. , *Catalysis Today,* **2007**, 126, 27.

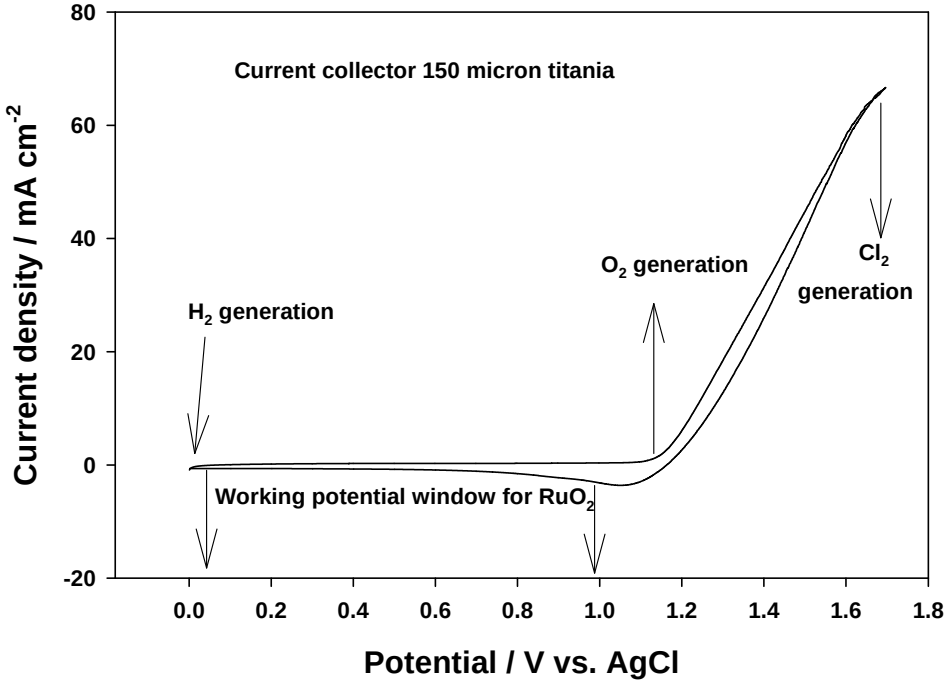

Fig.1 Evaluation of working potential window with respect to hydrogen, oxygen and chlorine evolution reaction

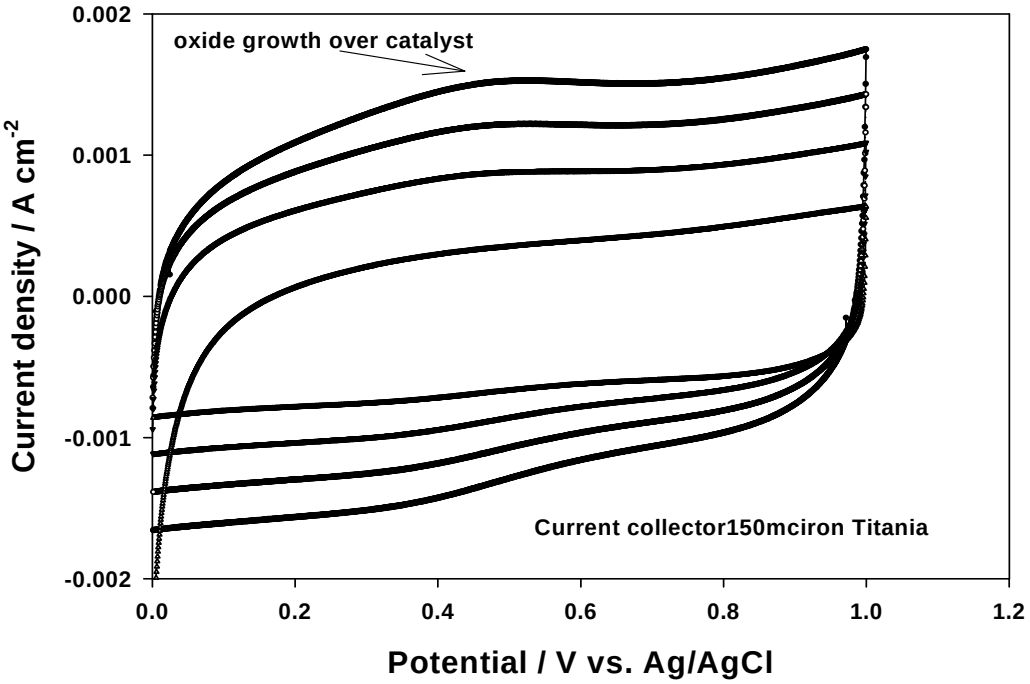

Fig.2 Cyclic voltammograms for RuO_2 at various scan rate

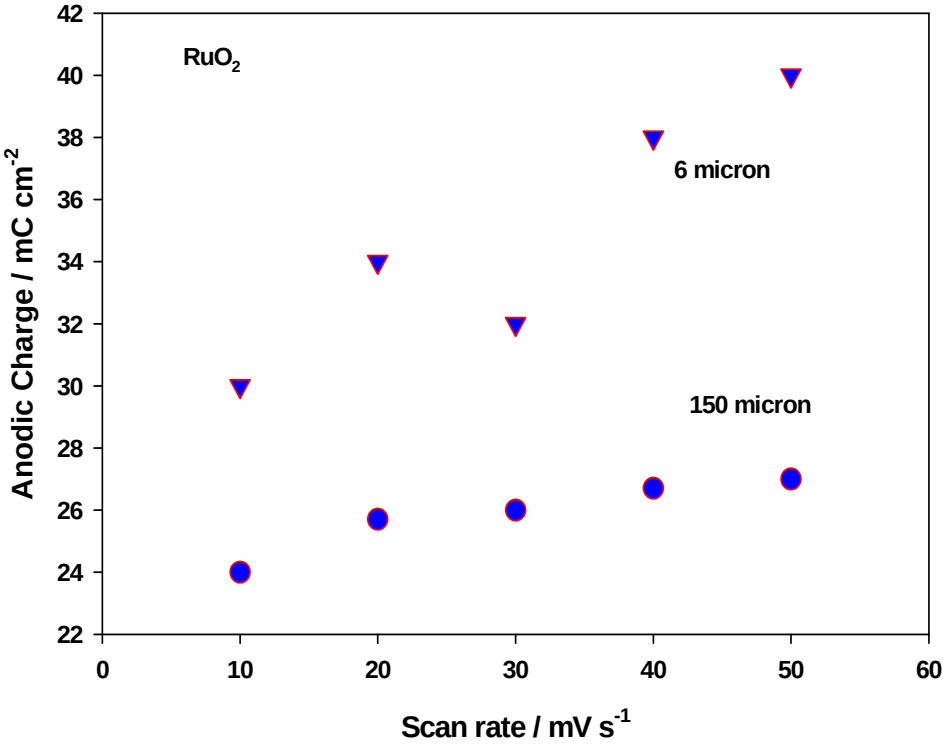

Fig.3 A comparison of anodic charge for RuO_2 coated over 6 micron and 150 micron titania.

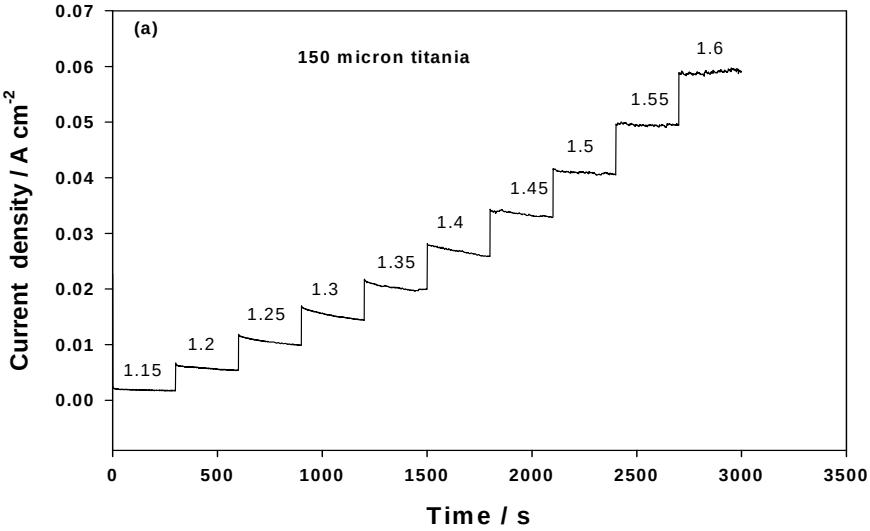

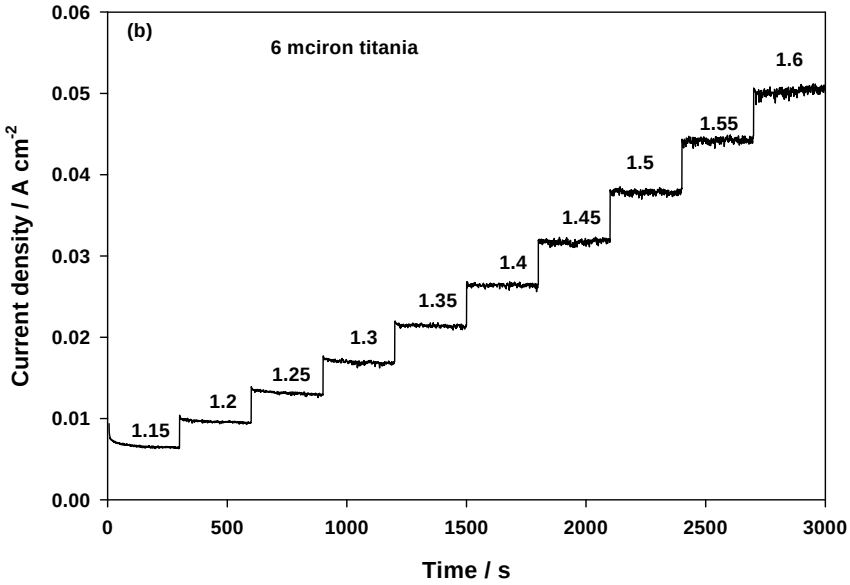

Fig.4 Chronoamperometry experiment was performed to follow up the chlorine generation reaction, with catalyst RuO_2 coated over 150 and 6 micron titanium.

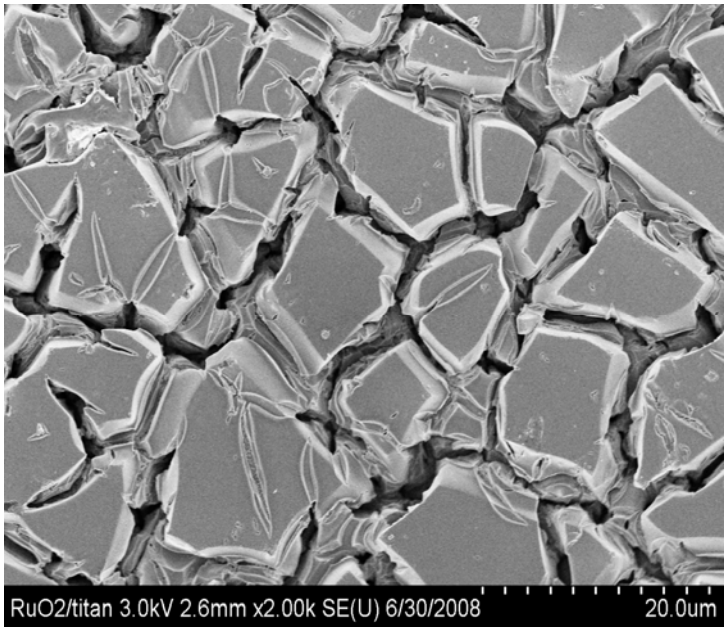

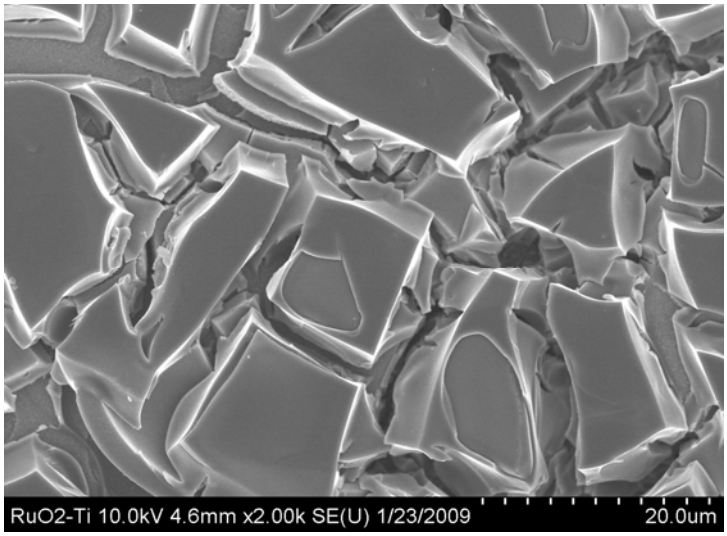

Fig.5 Two different micrograms of RuO_2 over two different titanium current collector.

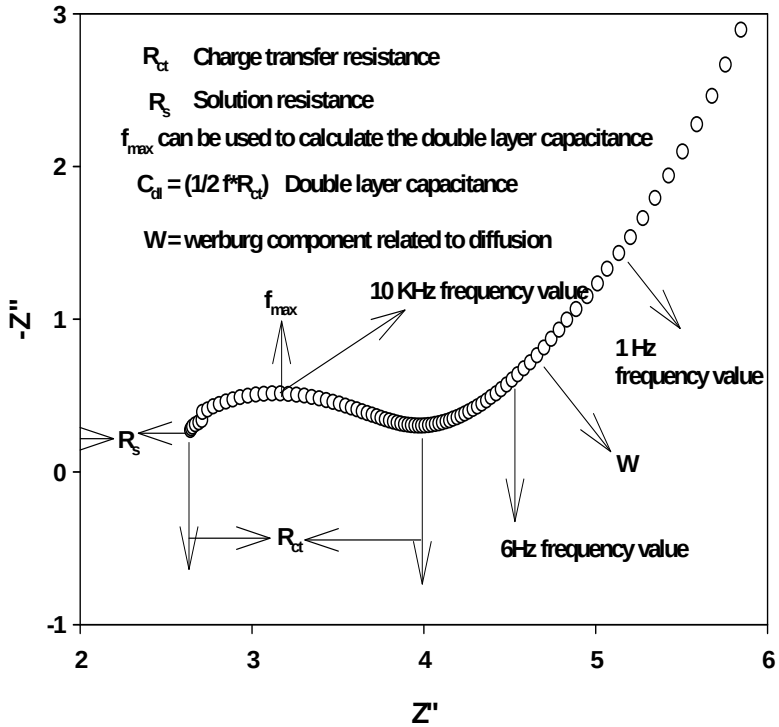

Fig. 6 Model impedance diagram, Nyquist plot for Z(imp) and Z(real) and also a model for double layer.

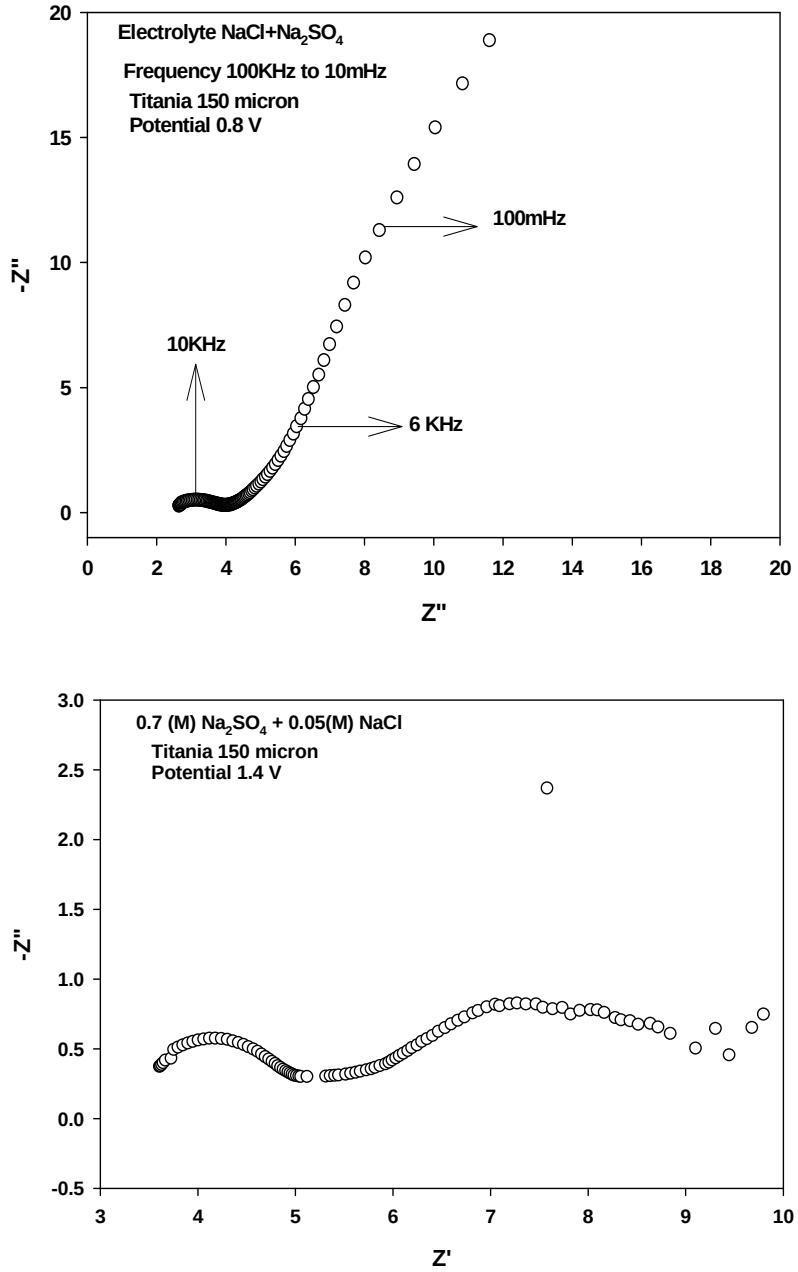

Fig.7 Nyquist spectrum for RuO_2 obtained at same potential value for 150 micron thickness of titanium.

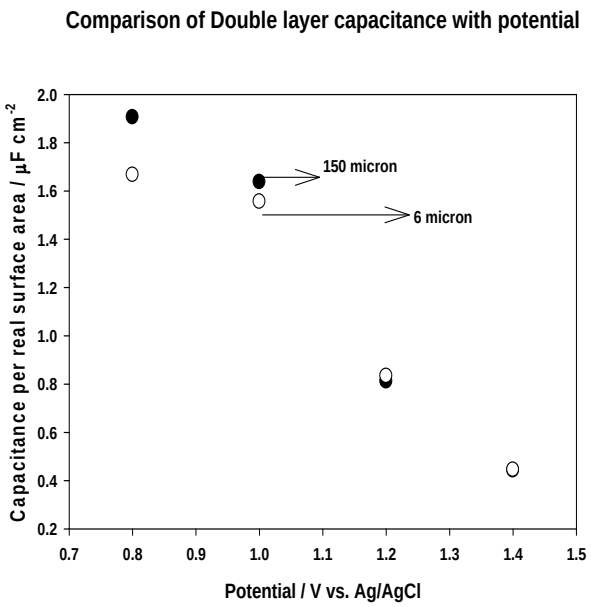

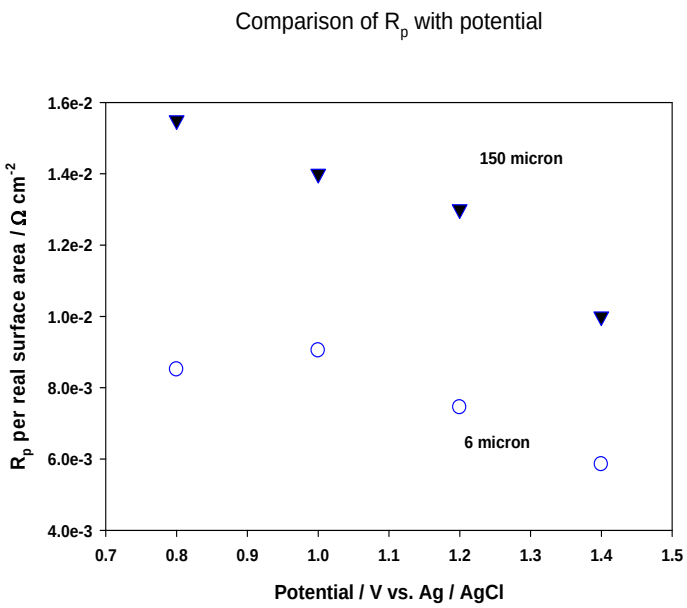

Fig.8 Change of double layer capacitance and charge transfer resistance obtained from Nyquits spectrum for two different thickness of titanium current collector.

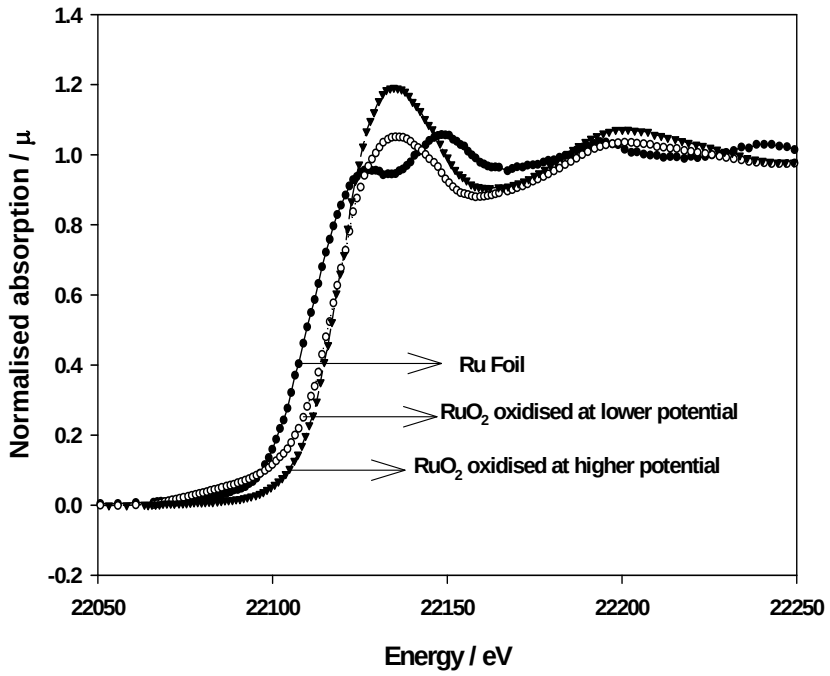

Fig.9 XANES spectra for both samples and Ru foil.

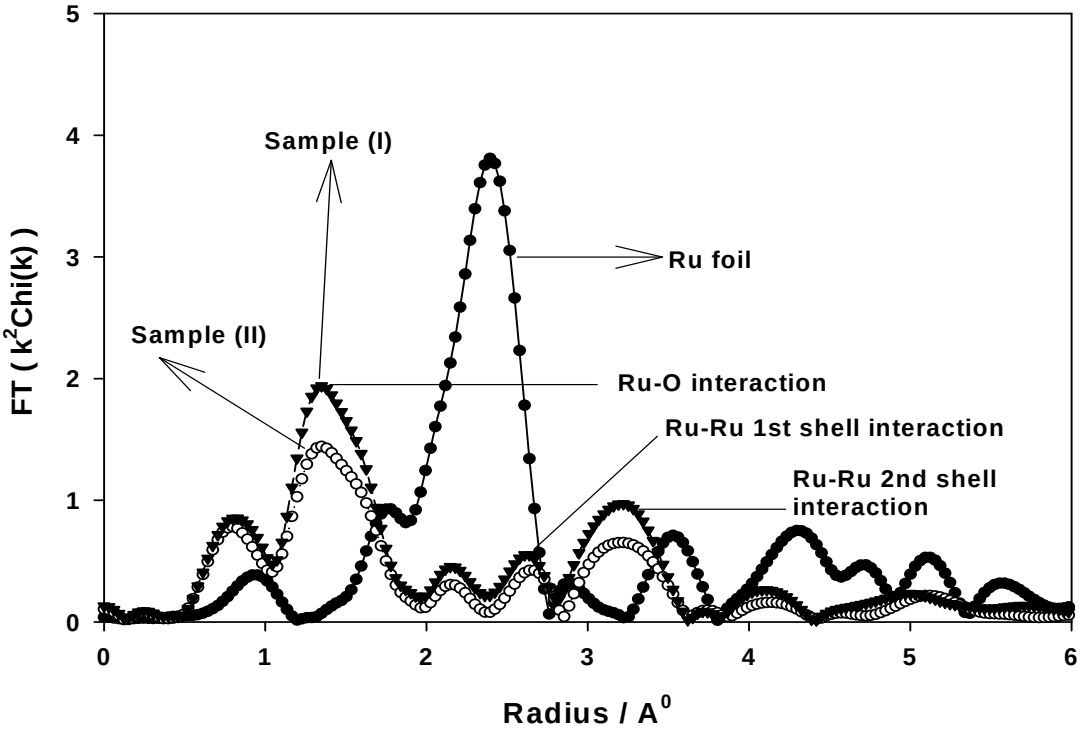

Fig.10 Pseudo radial distribution function for both sample and Ru foil.

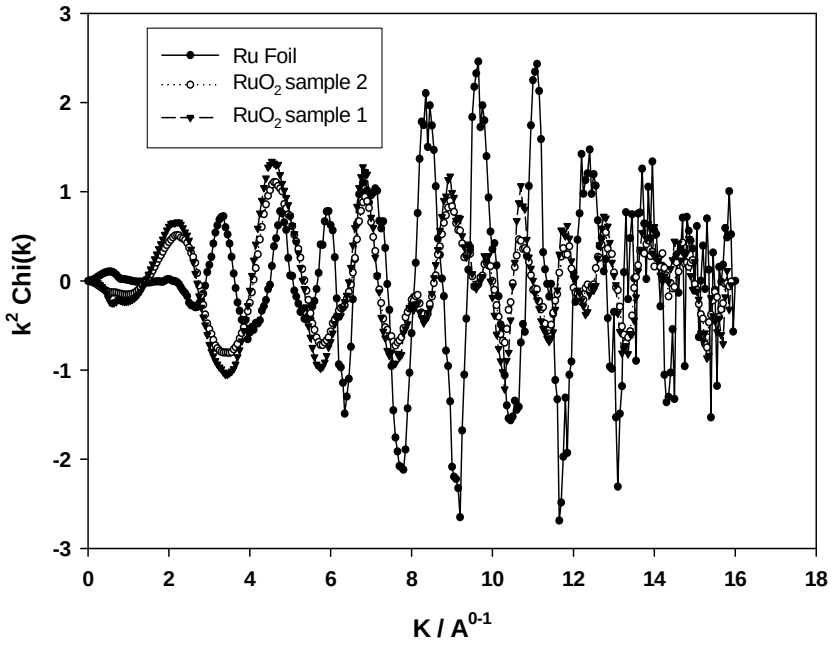

Fig. 11 Comparison of oscillatory chi(k) function for samples and Ru foil.

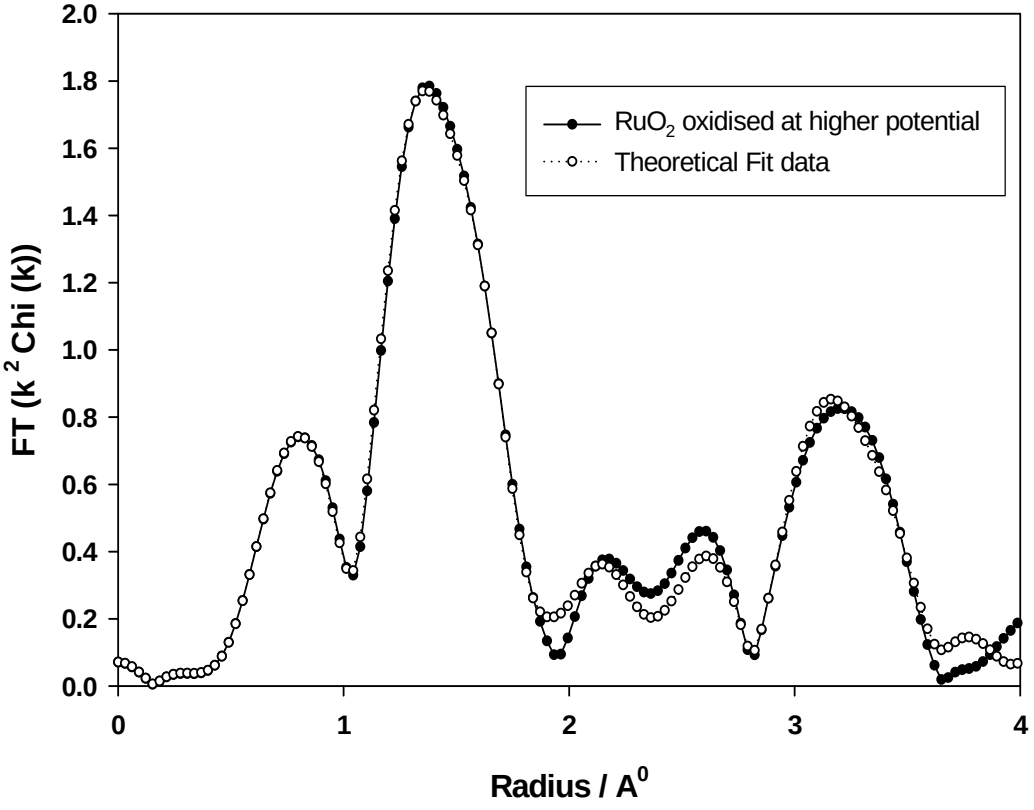

Fig.12 Comparison of theoretical fit data with the data obtained from sample I.

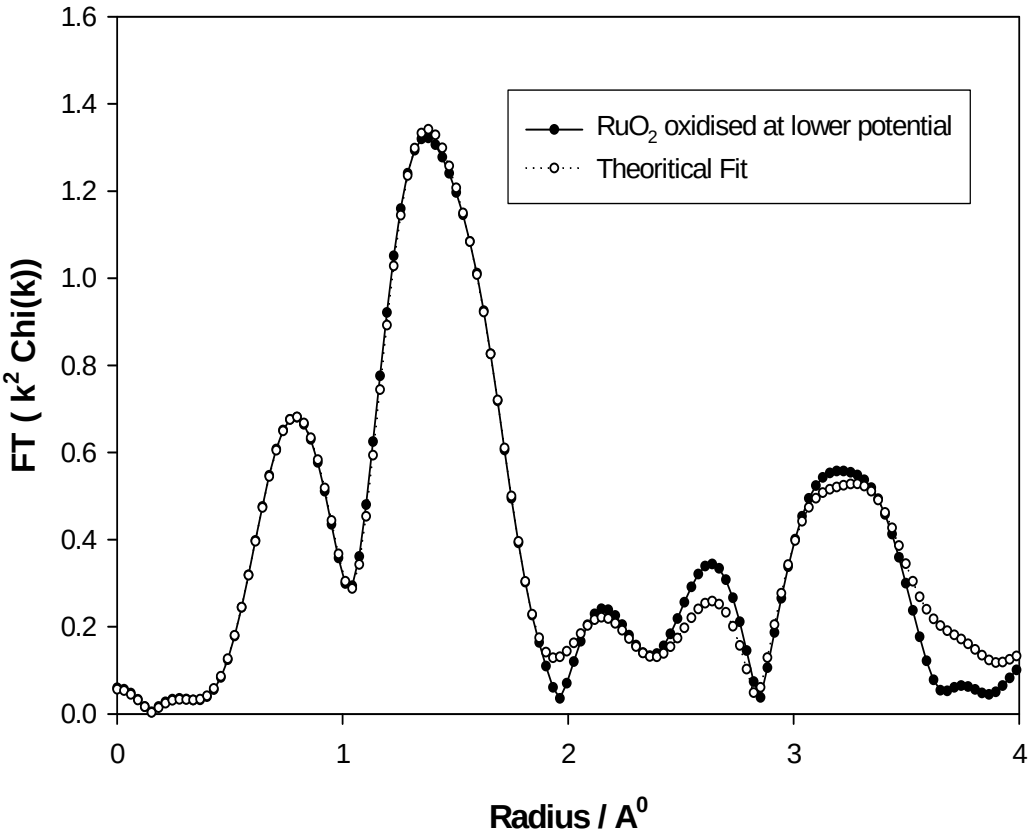

Fig.13 Comparison of theoretical fit data with the data obtained from sample II

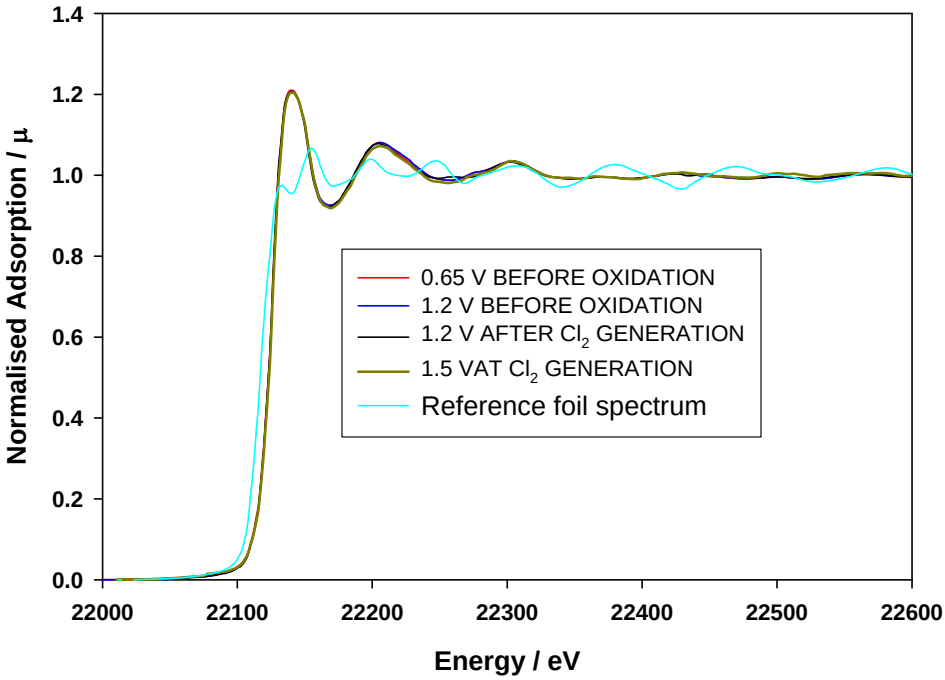

Fig. 14 In-situ XANES results for RuO_2 coated over 6 micron Titanium, spectra taken at different potential values.

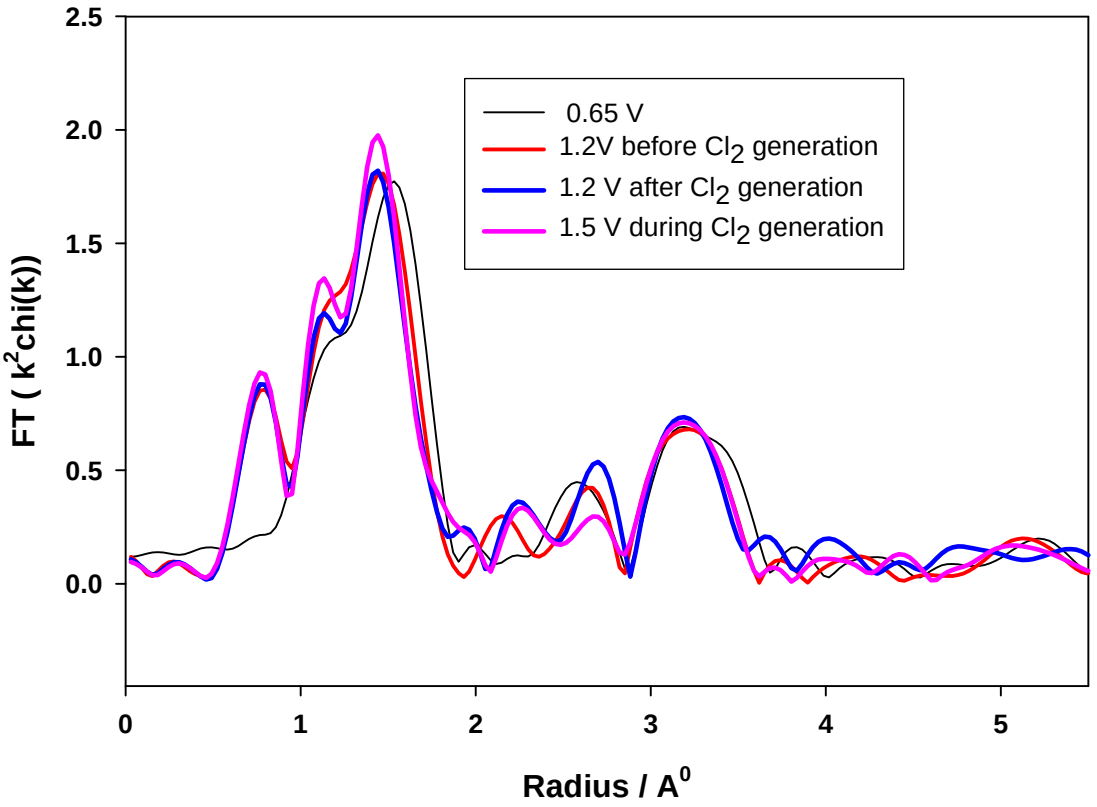

Fig. 15 Pseudo radial function derived from in-situ experiment for RuO_2 sample coated over six micron titanium.

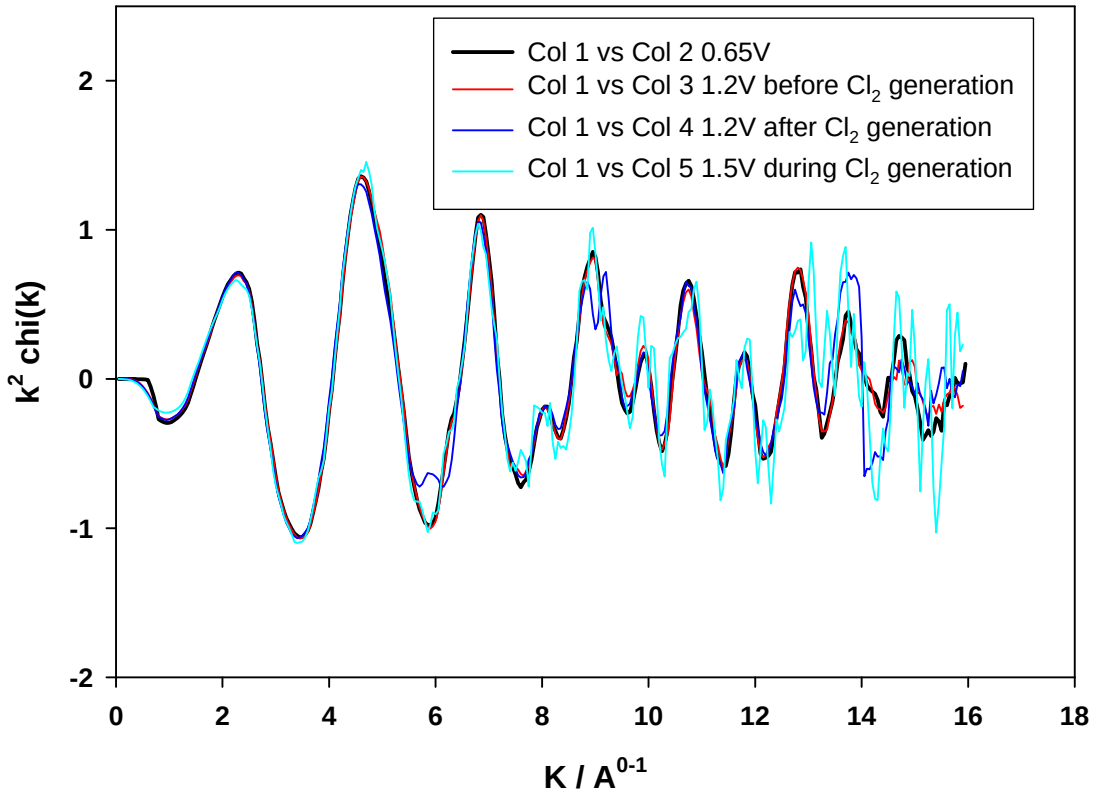

Fig. 16 Comparison of oscillatory chi(k) function for samples obtained at various operating potential.

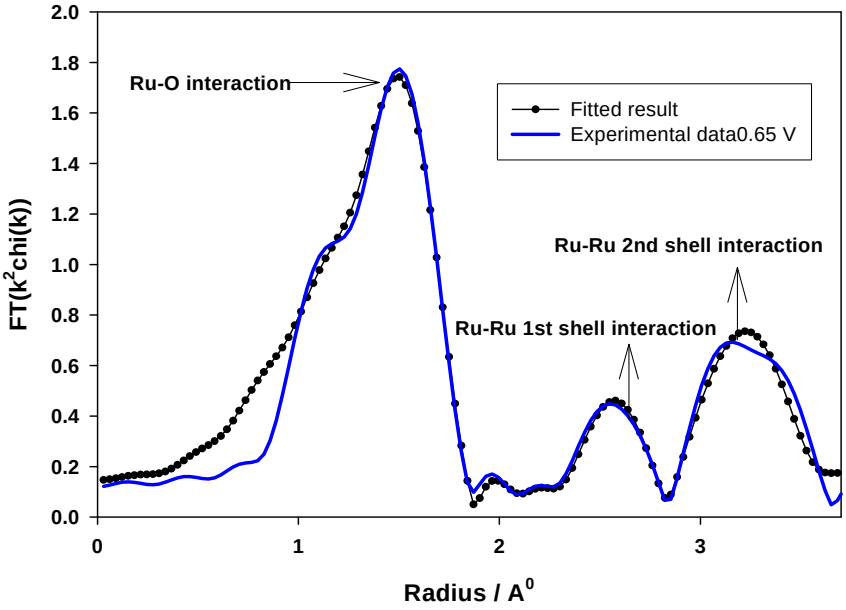

Fig. 17 Comparison of theoretical fit and experimental results obtained at operating potential 0.65 V with respect to Ag/AgCl.